

Indentation fatigue

A simple cyclic Hertzian test for measuring damage accumulation in polycrystalline ceramics

By FERNANDO GUIBERTEAU[†], NITIN P. PADTURE[‡], HONGDA CAI[‡]
and BRIAN R. LAWN

Materials Science and Engineering Laboratory,
National Institute of Standards and Technology,
Gaithersburg, Maryland 20899, USA

[Received 4 February 1993 and accepted 17 May 1993]

ABSTRACT

A simple Hertzian contact procedure for investigating cyclic fatigue damage in brittle polycrystalline ceramics is described. Repeat loading of a spherical indenter on a coarse alumina ceramic produces cumulative mechanical damage. The mode of damage is one of deformation-induced intergranular microfracture, leading ultimately at large numbers of cycles and high contact pressures to severe grain dislodgement. In contrast to the classical Hertzian cone cracks that form in more homogeneous materials in the regions of tensile stress *outside* the contact circle, the damage in the coarse-grain alumina develops in a zone of high shear stress and hydrostatic compression *beneath* the contact circle. The fatigue damage is evident in inert environments, confirming the mechanical nature of the process, although exposure to moisture accelerates the effect. The relatively modest degradation in failure stress with number of repeat contacts for indented flexure specimens suggests that conventional strength and toughness testing procedures may not always provide sensitive indications of the extent of damage that can be incurred in concentrated loading.

§1. INTRODUCTION

Strength and toughness properties in monotonic loading have been extensively investigated in ceramics. Special interest has recently been shown in polycrystalline materials with enhanced toughening from crack bridging, including various types of monophase and multi-phase composites (Knehan and Steinbrech 1983, Swanson, Fairbanks, Lawn, Mai and Hockey 1987, Bennison and Lawn 1989a, b, Chantikul, Bennison and Lawn 1990, Bennison, Rödel, Lathabai, Chantikul and Lawn 1991, Padture *et al.* 1991, Braun, Bennison and Lawn 1992a, b). Bridging leads to toughness-curve (*T*-curve, or *R*-curve) behaviour, with desirable long-crack flaw tolerance. It is enhanced by internal stresses, e.g. from thermal expansion anisotropy (TEA) mismatch, and is more pronounced in coarser grain microstructures.

However, the same internal stresses responsible for enhanced bridging in the long-crack domain can lead to deleterious short-crack properties, because of premature grain boundary cracking at tensile facets. Wear studies afford an illustrative precedent.

[†] Guest Scientist, from Departamento de Física, Universidad de Extremadura, 06071-Badajoz, Spain.

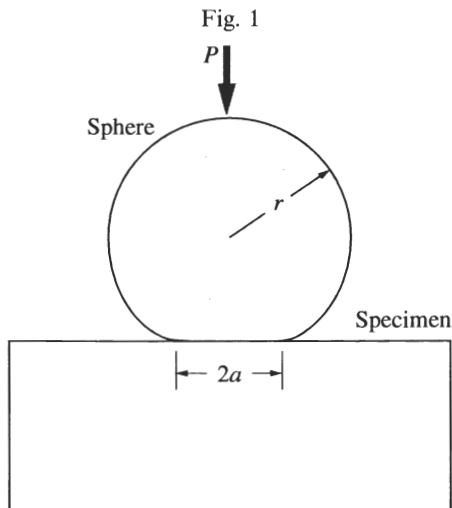
[‡] Guest Scientist, from Department of Materials Science and Engineering, Lehigh University, Bethlehem, Pennsylvania 18015, USA.

In alumina, increasing the grain size increases the long-crack toughness (Chantikul *et al.* 1990), but reduces the resistance to microfracture-assisted wear from multi-pass sliding contacts (Cho, Hockey, Lawn and Bennison 1989, Cho, Moon, Hockey and Hsu 1992). The mechanism of material degradation is an abrupt rise in grain boundary microfracture after an incubation wear period, from the steady augmentation of internal stresses by deformation-accumulation stresses (Ajayi and Ludema 1988, Cho *et al.* 1989). It is not just fracture mechanics, but also precursor damage mechanics, that govern 'failure' events.

These remarks are particularly relevant to the potential response of tough ceramics in repeated loading, i.e. cyclic fatigue (Ritchie 1988, Suresh 1991). Traditional cyclic fatigue tests are conducted on specimens with long cracks. Such tests are expensive, difficult, and labour intensive. They require testing machines with demanding load control over extended periods. An even more compelling criticism is that it is not generally valid to extrapolate long-crack results back to the short-crack region, where strength is determined, since for a given material the extreme-region toughness values are often inversely related—i.e. the toughness curves for different grain sizes tend to cross each other (Chantikul *et al.* 1990). This last point is especially pertinent in view of the fact that many ceramic components in service experience concentrated contact stresses (Lawn and Wilshaw 1975) at the microstructural level, rather than macroscopically distributed stresses of the type simulated in conventional crack propagation and strength tests. Questions then arise as to the mechanics of 'failure' in such concentrated loading conditions, and their relevance to fatigue properties.

In this study we propose a simple new procedure for studying the fatigue properties of brittle polycrystalline ceramics. We use an indenter to apply a concentrated load on flat alumina surfaces, and examine the ensuing damage patterns as a function of number of cycles. Some contact damage studies on polycrystalline ceramics have previously been made with 'sharp' fixed-profile indenters (Lawn and Wilshaw 1975) (e.g. Vickers or Knoop pyramids, or Rockwell cones) where the contact pressure (i.e. the 'hardness') is effectively independent of load (Sperisen, Carry and Mocellin 1986, Makino, Kamiya and Wada 1988, 1991, Howes 1990, Reece and Guiu 1991). However, although sharp indenters usefully reveal the microstructural nature of the damage process, they produce virtually 'saturated' deformation at first contact, and are therefore not ideally suited for examining damage *evolution*. Where they have been used in repeated loading (Howes 1990, Reece and Guiu 1991), such indentation experiments reveal only slight fatigue tendencies.

Accordingly, in the present study we use the spherical indenter configuration of fig. 1, where the contact pressure increases monotonically with load from zero at first contact. In its initial stages of loading the stress field is purely elastic, i.e. the classical Hertzian stress field (Hertz 1896, Johnson 1985); the indentation is said to be blunt (Lawn and Wilshaw 1975). Beyond a critical load the material undergoes irreversible deformation and/or fracture. In well-behaved, highly brittle materials like silicate glasses, single crystals, and ultra-fine-grain polycrystals a well-defined cone-shaped crack, the Hertzian fracture, runs around the contact circle and spreads downward and outward into the material. This kind of fracture has received extensive attention in the literature (Frank and Lawn 1967, Lawn 1968, Langitan and Lawn 1969, Lawn and Wilshaw 1975, Lawn and Marshall 1978). In softer, less brittle materials like most metals (Tabor 1951) and lithium fluoride monocrystals (Swain and Lawn 1969) the material deforms plastically beyond the elastic limit; cracks, when they do ultimately develop, take on more of the form of the *radial* and *lateral* geometries characteristic of



Schematic diagram of indentation with hard elastic sphere of radius r , load P , on flat brittle surface. Loads are made in single (static test) or multiple (fatigue test) cycles.

sharp indenters (Lawn and Swain 1975, Lawn and Wilshaw 1975). This latter kind of deformation-initiated fracture can also be generated in more brittle materials by using indenters of smaller radius (Swain and Hagan 1976)—there is a ‘size effect’ in the contact process, in which the pattern undergoes a transition from ‘blunt’ to ‘sharp’ as the sphere radius is diminished (Lawn and Wilshaw 1975, Lawn 1993).

We shall see that in the tougher, coarser polycrystalline bridging ceramics of interest to us here the fracture pattern is more complex than those discussed above, involving deformation and fracture at the microstructural level. We shall also demonstrate that the spherical-indenter test provides a useful and uncommonly sensitive tool for investigating such damage.

§2. EXPERIMENTAL METHOD

The material chosen for the main focus of the present study was a high-purity commercial alumina with grain size $23\ \mu\text{m}$.† This is sufficiently coarse that the material has a significant toughness-curve (Bennison and Lawn 1989b, Chantikul *et al.* 1990, Braun, Bennison and Lawn 1992a). The material is similar to that used in an earlier fatigue study (Lathabai, Mai and Lawn 1989). In that earlier study the specimens were in the form of discs, each containing a well-developed Vickers indentation crack. Biaxial flexure tests revealed no measurable strength degradation from cyclic loading to $>10^5$ cycles.‡

A fine-grain alumina (grain size $2.5\ \mu\text{m}$) with conventional Hertzian fracture properties (§3.1.) was used as a control material with an effectively single-valued toughness (Braun *et al.* 1992a).

The alumina specimens were obtained as discs 30 nm diameter and 4 nm thick. Their surfaces were polished to a final finish with $1\ \mu\text{m}$ diamond grit. Indentations were

† Vistal grade Al_2O_3 , Coors Ceramics Co., Golden CO, USA.

‡ Later tests in a similar alumina of grain sizes $35\ \mu\text{m}$ did reveal a measurable degradation, $<20\%$, over $>10^7$ cycles (Lathabai, Rödel and Lawn 1991).

made with tungsten carbide spheres, radii $r = 1.98, 3.18, 4.76, 7.94$ and 12.70 mm. Loads in the range $P = 0$ to 3500 N were delivered using crosshead testing machines† at constant displacement rates. The practical loads achievable at smaller radii were ultimately limited by permanent deformation of the WC spheres themselves (see § 3.2). Cycling between zero and specified maximum loads was conducted at frequencies of 1 Hz ('fast cycle') and 0.002 Hz ('slow cycle'). A few control static tests were run over a prolonged hold time at maximum load. The indentation test environment was either nitrogen gas (relative humidity $< 1.5\%$), laboratory ambient (humidity $40\text{--}50\%$), or water. Some specimens were coated with gold *prior* to indentation so that the contact radius might be determined as a function of applied load from the residual surface trace, and the contact pressure thereby determined (§ 3.2).

Reflection optical microscopy was used to examine the indented surfaces. The presence of surface damage was detected by coating the surfaces with gold *after* indentation and viewing in Nomarski interference contrast. Subsurface damage in the translucent coarse alumina was most readily observable in dark-field illumination. Some specimens were sectioned through the indentations to examine the extent of the subsurface damage, by cutting adjacent to the indentation sites and grinding and polishing down to the contact diameter.

Flexure tests were carried out on a batch of indented discs to determine the effect of cyclic degradation on strength. In these tests each disc contained a single cyclic Hertzian indentation at its centre. The discs were broken in biaxial flexure, using a flat circular punch of diameter 6 mm on a three-point support of diameter 22 mm. Prior to flexure the indentations were covered with a drop of silicone oil, and the specimens broken within a load time < 10 ms, to determine 'inert strengths'.

§ 3. RESULTS

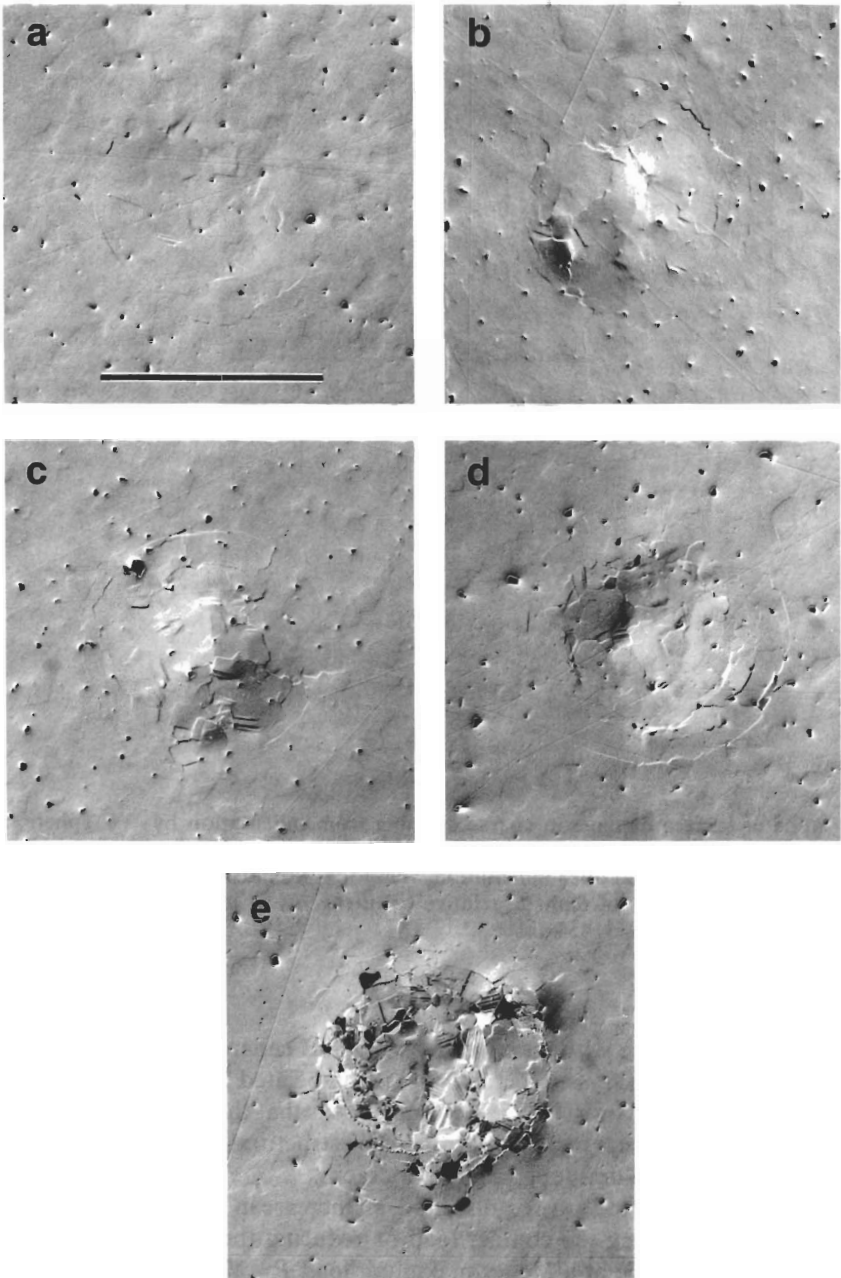
3.1. *Damage of indented alumina surfaces*

The evolution of cyclic indentation damage in the coarse grain alumina specimens for indentations in nitrogen gas is apparent in the sequence of fig. 2. The sequence represents an increasing number of cycles, $n = 1, 10, 100, 1000$ and $10\,000$, at frequency 1 Hz, sphere radius $r = 3.18$ mm and maximum load $P = 1000$ N. These indentation conditions correspond to the first detectable onset of single-cycle damage. A progressive accumulation of damage with number of cycles is evident in the sequence. Since dry nitrogen is an effectively inert environment, one may assert that the cumulative damage process is driven essentially by *mechanical* forces, as distinct from *chemical* forces. Nevertheless fig. 3, which shows micrographs taken under the same indentation conditions as in fig. 2(e) (i.e. $n = 10\,000$ cycles) but in air and water, indicates that the role of chemistry, while not primary, is not benign in the final damage evolution.

Closer inspection of the micrographs in figs. 2 and 3 provides some insight into the nature of the damage. At some of the indentations, segmented circular crack traces are apparent in the outer regions of the damage pattern, indicative of the formation of 'partial' cone fractures outside an expanding contact circle (final diameter indicated by marker in figs.) (Lawn and Wilshaw 1975). The incidence of these fractures does not increase markedly with the number of cycles. On the other hand the damage within the inner contact area, manifested macroscopically as an ever-deepening residual contact

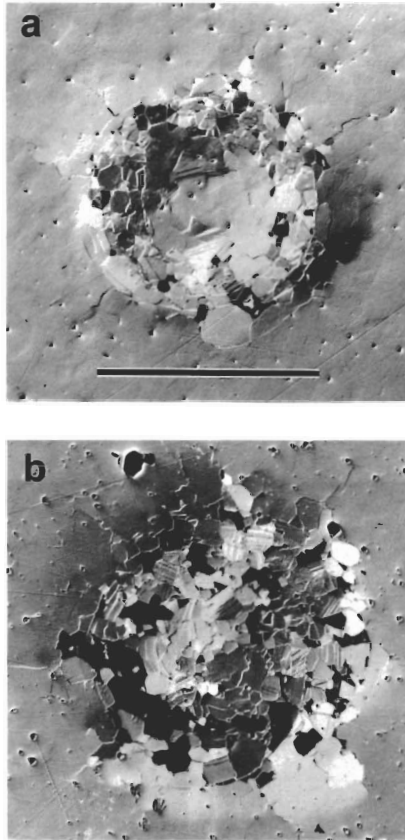
† Instron Universal Screw-Driven Testing Machine 1122 (slow-cycle tests) and Digital Servo-Hydraulic Testing Machine 8502 (fast-cycle tests), Instron Corp., Canton, MA, USA.

Fig. 2



Micrographs of surface damage in coarse alumina (grain size $23\ \mu\text{m}$) from indentation by WC sphere, radius $r = 3.18\ \text{mm}$, at load $P = 1000\ \text{N}$, in dry nitrogen gas. Number of cycles n , (a) 1, (b) 10, (c) 100, (d) 1000, (e) 10000, frequency 1 Hz. Surfaces gold coated after indentation, viewed in Nomarski interference illumination. Marker denotes contact diameter, $2a = 454\ \mu\text{m}$.

Fig. 3

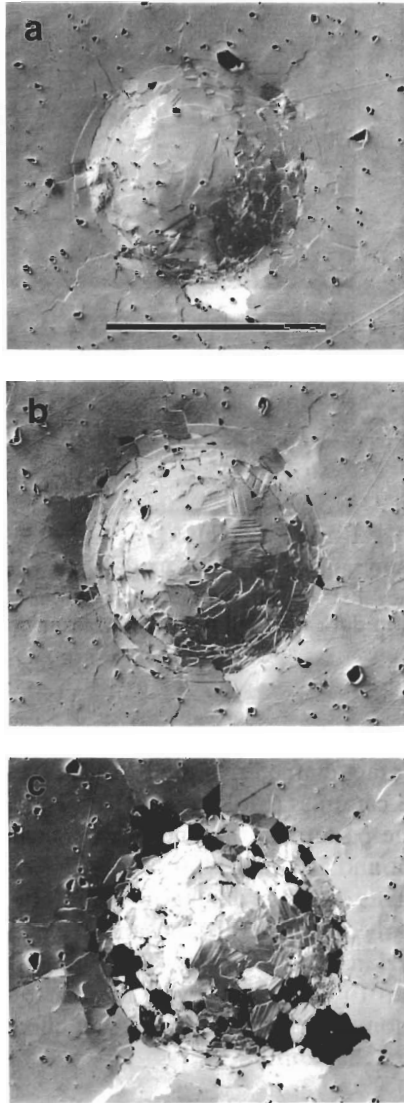


Micrographs of surface damage in coarse alumina from indentation by WC sphere, radius $r = 3.18$ mm, load $P = 1000$ N, $n = 10\,000$ cycles, frequency 1 Hz. Tests in (a) air, (b) water. Surfaces gold coated after indentation, viewed in Nomarski interference illumination. Note enhancement of damage relative to nitrogen test in fig. 2(e). Marker denotes contact diameter, $2a = 454$ μm .

impression, does increase with number of cycles. This enhanced damage is characterized by *intergrain* boundary microcracking, and associated *intragrain* deformation in the form of twin or slip bands. Hence it would appear that the fatigue process involves deformation-induced crack initiation at the microstructural level, rather than enhanced propagation of well-developed Hertzian cracks.

As we shall see in the following subsection, an increase in indentation pressure may be rendered by increasing the contact load or reducing the sphere radius. Figure 4 shows indentations made at a higher maximum load $P = 2000$ N and smaller sphere radius $r = 1.98$ mm, for $n = 1$ (fig. 4(a)) and 10 (fig. 4(c)), at frequency 0.002 Hz, in water. For comparison, the figure includes an indentation held at maximum load for an extended duration equal to the total time taken by ten normal cycles (fig. 4(b)). We observe a conspicuous enhancement in surface damage after the cyclic loading, but *not* after the static loading. This sequence reaffirms the existence of a true mechanical fatigue effect—the results cannot be simply interpreted as the integration over time—

Fig. 4

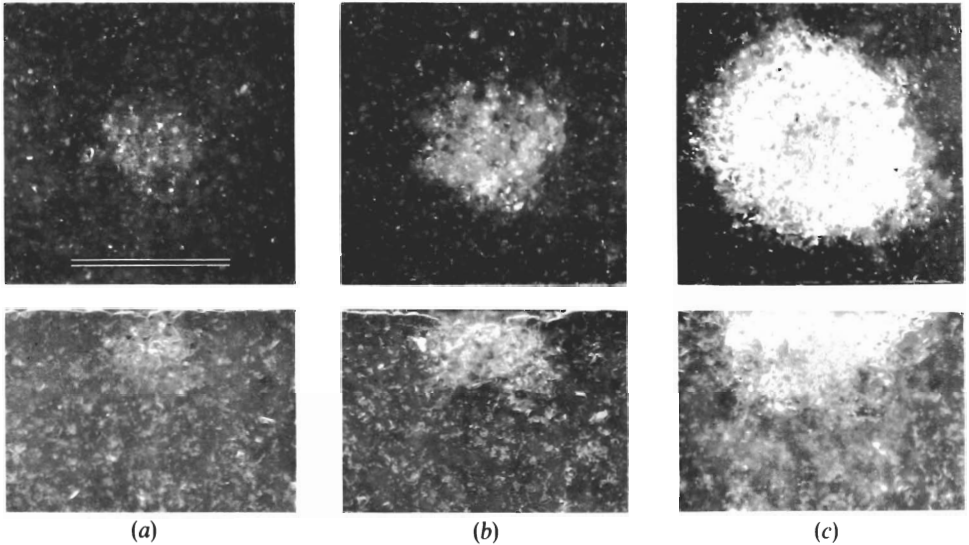


Micrographs of surface damage in coarse alumina, WC sphere radius $r=1.98$ mm, load $P=2000$ N, in water: (a) 1 cycle at 0.002 Hz; (b) static test at same peak load with hold time equal to total duration of test (c); (c) 10 cycles at 0.002 Hz. Surfaces gold coated after indentation, viewed in Nomarski interference illumination. Marker denotes contact diameter, $2a=500$ μm .

dependent slow crack growth, because the prolonged hold time at maximum load does not significantly enhance the damage relative to the cyclic test.

The cause of the residual impression is evident in the dark field micrographs of fig. 5 (upper views), of indentations in air at $n=1, 100, 10\,000$ cycles. The micrographs show enhanced specular scattering from below the contact area, indicating the presence of a pervasive subsurface microcracking crush zone. Section views through such indentations (lower views) indicate that the microcrack zones initiate beneath the actual contact surface and, with increasing load, extend upward to the surface and downward

Fig. 5



Damage in coarse alumina, WC sphere radius $r = 3.18$ mm, load $P = 1000$ N: (a) 1, (b) 100, (c) 10000 cycles, frequency 1 Hz, in air. Upper micrographs surface views, lower micrographs section views, in dark field illumination. Marker denotes contact diameter, $2a = 454$ μm .

to a depth of order one contact diameter. Similar subsurface damage zones have been observed in silicon nitride ceramics (Makino *et al.* 1991).

An indentation damage pattern in the fine-grain *control* alumina, for $n = 10000$ cycles at 1 Hz, $r = 3.18$ mm and $P = 1000$ N, in air, is shown in fig. 6. Relative to its coarse-grain counterpart in fig. 3 (a), the damage is slight. The incidence of any damage at all becomes apparent only after several thousand cycles; and, when it does occur, assumes the classical Hertzian cone geometry. There is no detectable microcracking within the contact area up to the 10000 cycle limit in our experiments. There is therefore a clear implication of a microstructure size effect in the damage process responsible for the fatigue behaviour.

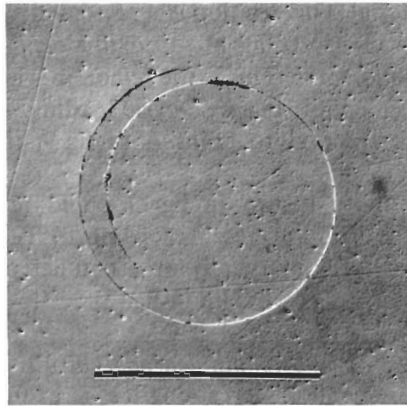
3.2. Indentation stress-strain curve

Consider again the sphere, radius r , load P , on a flat specimen surface, in the schematic diagram of fig. 1. We can define useful scaling quantities for the contact field, regardless of whether the deformation is elastic or inelastic (Tabor 1951, Swain and Lawn 1969). The magnitude of the stress field scales with the mean indentation pressure,

$$p_0 = P/\pi a^2. \quad (1)$$

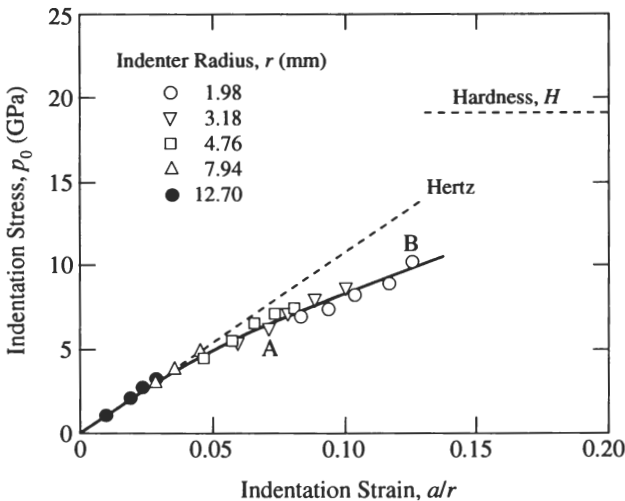
Likewise, from geometrical similarity, the magnitude of the strain field scales with a/r . Hence we may determine a characteristic indentation stress-strain curve $p_0(a/r)$ for a given material, independent of sphere size. Such curves have been previously determined for lithium fluoride single crystals (Swain and Lawn 1969) and silicate glasses (Swain and Hagan 1976).

Fig. 6



Micrograph of surface damage in fine alumina (grain size $2.5\ \mu\text{m}$), produced by WC sphere, radius $r = 3.18\ \text{mm}$, at load $P = 1000\ \text{N}$, $n = 10\ 000$ cycles, in air. Surfaces gold coated after indentation, viewed in Nomarski interference illumination. Marker denotes contact diameter, $2a = 454\ \mu\text{m}$ (cf. fig. 3 (a)).

Fig. 7



Indentation stress–strain curve for single-cycle contacts in coarse alumina, in air, using spheres of different radius as indicated. Dashed line is Hertzian elastic response, eqn. (2). Point A corresponds to loading conditions in figs. 2 and 3, B to conditions in fig. 4.

We generate appropriate $p_0(a/r)$ data points for our coarse grain alumina in fig. 7, from measurements of a at each value of P from single-cycle tests in air using spheres of specified radii r . We see that for a given sphere radius the indentation pressure initially rises linearly, in accord with the Hertzian theory of elastic contact (Swain and Lawn 1969):

$$p_0 = (3E/4\pi k)(a/r), \tag{2}$$

where $E = 393\ \text{GPa}$ is Young's modulus of the alumina; the constant

$$k = (9/16)[(1 - \nu^2) + (1 - \nu'^2)E/E'] = 0.88$$

for tungsten carbide on alumina, with ν Poisson's ratio and the prime notation denoting the indenter material. This relation is represented as the dashed line in fig. 7.

The data deviate below the Hertz line at approximately $p_0 \approx 3\text{--}5$ GPa, as indicated by the empirically fitted solid curve. This is the region in which deformation-induced microcracking becomes perceptible in single-cycle loading. For instance, the indentations in figs. 2 and 3 correspond to point A in fig. 7; the indentations in fig. 4 correspond to point B.

Higher stresses than those shown in fig. 7 could not be achieved without permanently deforming the WC spheres. According to Tabor (1951), an isotropic indenting sphere should deform plastically at a contact pressure ≈ 0.4 times the hardness, which corresponds to $p_0 \approx 8$ GPa in fig. 7.

3.3. Strength degradation

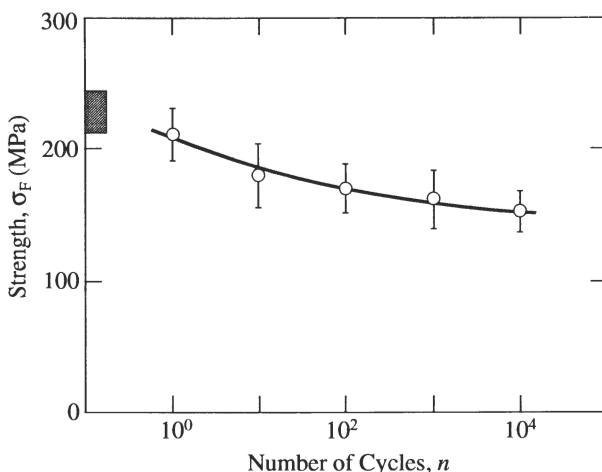
Results from the measurements of inert strength σ_F as a function of number of cycles n in air are plotted in fig. 8. The indentations in these experiments correspond to the loading conditions A in fig. 7, i.e. just beyond the point of first perceptible deviation from the Hertz line, so as to allow for maximum development of mechanical damage during cycling.

Relative to surfaces *without* indentations (hatched box at left in fig. 8), we see that measurable strength degradation is achieved in the first cycle. For repeat indentations, the degradation relative to specimens with a single cycle is $< 30\%$ over $1\text{--}10^4$ cycles. In view of the strong damage buildup apparent in figs. 2–5, this strength fall-off is relatively modest.

§4. DISCUSSION

We have demonstrated substantial fatigue effects in a coarse alumina ceramic using a Hertzian contact test. Microscopic examination of the contact sites reveals damage

Fig. 8



Strength of coarse alumina as function of number of cycles after indentation in air with sphere radius $r = 3.18$ mm, load $P = 1000$ N, frequency 1 Hz. Each datum point mean and standard deviation, four specimens. Hatched box at left axis represents breaks from specimens without indentations.

accumulation with increasing number of cycles. The test configuration is simple, requiring only a hard sphere and a smooth flat specimen surface, without the need for the fabrication of expensive, long-crack specimens. One still requires a testing machine for delivering the cyclic loading; however, in favourable cases, e.g. fig. 4, a conventional low-frequency machine may be sufficient to demonstrate the effect.

Strength tests provide a quantitative measure of the severity of accumulated damage. In fig. 8 the degradation relative to first-cycle contact is almost 30% over 10^4 cycles in air. However, strength degradation does not reflect the severity of damage accumulation observed in the micrographs of figs. 2–5.† Strength depends not on the *density*, but rather the *size*, of the flaws; and even this latter dependence is somewhat tempered by the existence of a toughness-curve (Lathabai *et al.* 1989). Flaw density is of much greater influence in wear properties. A similar insensitivity in strength characteristics has been demonstrated in *translating* sphere tests on glass, where an increased friction coefficient produces substantially enhanced contact damage but has relatively small influence on the failure stresses of the contacted surfaces (Lawn, Wiederhorn and Roberts 1984). Again, the implication is that strength (and, by association, toughness) measurements may not always be the most practical measure of damage accumulation in contact fatigue configurations. In this context, it may be noted that the present concentrated-load tests deliver much higher stresses over a much smaller area (typically 5 GPa over 0.1 mm^2) than in conventional strength tests (typically 500 MPa over 100 mm^2). Alternative tests for quantifying accumulated damage during contact history, e.g. acoustic emission (Sperisen *et al.* 1986), might provide more relevant quantitative information.

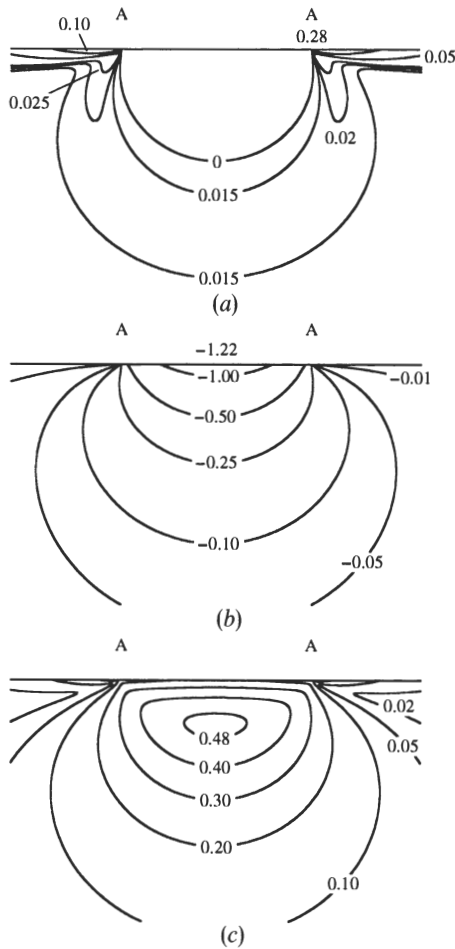
As to indenter geometry, the 'blunt' contact typified by the Hertzian configuration is especially favoured for following the evolution of damage, because the contact pressure increases monotonically up the $p_0(a/r)$ curve in fig. 7, from linear elastic to the onset of first deformation and microcracking through to the fully elastic–plastic region. The same is not true of 'sharp' contacts with fixed-profile indenters, e.g. Vickers, because the contact pressure saturates at the hardness value H (load/projected contact area, horizontal dashed line in fig. 7) virtually at first contact.‡

The question as to the mode of cyclic fatigue in the alumina remains to be answered. It appears to be primarily mechanical rather than chemical. An important ingredient of any fatigue mode is the existence of some 'kinematic irreversibility of microscopic deformation' (Suresh 1991), so that hysteresis exists in the applied load–displacement function. In the present case the onset of intragrain deformation, coupled with ensuing microcracking, would appear to constitute the necessary basis for such irreversibility. But what are the basic elements of the deformation, and what stresses are needed to activate these elements? In single crystal sapphire, twinning and high-stress slip can occur at room temperature (Hockey 1971, Cannon 1984, Chan and Lawn 1988); in polycrystals, grain boundary stress concentrations from these shear elements, in combination with pre-existing thermal anisotropy stresses, can lead to premature grain

† This degradation is nevertheless considerably greater than that observed in a previous study on the same alumina in cyclic flexure testing *after* introduction of a single-cycle Vickers indentation (Lathabai *et al.* 1989).

‡ At the same time, the facility remains for the Hertzian test to simulate the broader features of sharp-indenter patterns, by virtue of an intrinsic size effect in the critical stress relation for cone fracture initiation: at sufficiently small sphere radius, the classical cone fracture is suppressed in favour of subsurface deformation, resulting in a kind of blunt–sharp, brittle–ductile transition (Lawn and Wilshaw 1975, Puttick 1979, Lawn 1993).

Fig. 9



Stress contours in Hertzian contact field, normalized by p_0 . (a) Principal tensile stress σ_1 , (b) hydrostatic stress $\frac{1}{3}(\sigma_1 + \sigma_2 + \sigma_3)$, and (c) principal shear stress $\frac{1}{2}(\sigma_1 - \sigma_3)$. Calculated using Poisson's ratio $\nu = 0.22$ for alumina. AA denotes contact diameter.

boundary microcracking. Again, wear studies with translating or rotating spherical indenters provide a precedent for this mechanism (Cho *et al.* 1989, 1992).

There is also the issue as to which stress component of the Hertzian field is responsible for initiating the damage. Recall in fig. 5 that the damage zone is located in a confined region beneath the contact area. An indication of the active component may be obtained from the Hertzian (elastic) stress field plots (Frank and Lawn, 1967, Lawn, Wilshaw and Hartley 1974, Lawn and Wilshaw 1975, Johnson 1985) in fig. 9. This diagram plots stress contours of the principal tensile stress [σ_1], hydrostatic stress [$\frac{1}{3}(\sigma_1 + \sigma_2 + \sigma_3)$], and principal shear stress [$\frac{1}{2}(\sigma_1 - \sigma_3)$]. Whereas the cone crack segments in figs. 2 and 3 form outside the contact area, i.e. where the normal stresses in fig. 9 (a) are mildly tensile (maximum $\approx 0.28p_0$ at contact circle), the subsurface microcrack zones form beneath the contact area, where the hydrostatic stresses in fig. 9 (b) are highly compressive (maximum $\approx -1.22p_0$ at the contact centre). However, the shear stresses

in fig. 9(c) also attain significant levels beneath the contact area (maximum $\approx 0.50p_0$ at depth $0.5a$ along contact axis). It is therefore most likely that those subsurface deformation processes (twinning and slip) ultimately responsible for the microcracking seen in fig. 5 are governed by the shear component of the stress field. Once such a deformation occurs, of course, the Hertzian elastic field description no longer prevails, and one must take into account the effect of irreversible processes on the stress-strain characteristics of the material (Lawn and Wilshaw 1975). In particular, the incidence of microcracking will inevitably dilate the material in the deformation zone, especially if local tensile TEA stresses are relaxed, setting up conditions for continued irreversibility in cyclic loading (Suresh 1991). The intrusion of water into the microcracks will only serve to enhance such irreversibility.

What are the materials implications of the observations in this study? How general are our results on coarse alumina? The comparatively small amount of damage observed in the fine-grain alumina in our studies implies the existence of potentially strong size effects from microstructural scaling. There is again the useful precedent from earlier wear studies on alumina using rotating spherical indenters, where the incubation time to effect a transition from deformation- to microfracture-controlled surface removal was found to increase dramatically at finer grain sizes (Cho *et al.* 1989). It would appear that the highest resistance to fatigue from damage accumulation may be achieved by refining grain size and by avoiding excessive internal residual stresses. Once more, such material requirements may well run counter to those for improving long-crack toughness (Bennison *et al.* 1989b, Chantikul *et al.* 1990, Lawn, Padture, Braun and Bennison 1993, Padture, Runyan, Bennison, Braun and Lawn 1993).

ACKNOWLEDGMENTS

Thanks are due to J. D. Sibold of Coors Ceramics Co. for providing the materials. Funding for this study was provided by the U.S. Air Force Office of Scientific Research. Financial support for F. G. from the Ministerio de Educación y Ciencia (DGICYT), Spain, is gratefully acknowledged.

REFERENCES

- AJAYI, O. O., and LUDEMA, K. C., 1988, *Wear*, **124**, 237.
 BENNISON, S. J., and LAWN, B. R., 1989a, *J. mater. Sci.*, **24**, 3169; 1989b, *Acta metall.*, **37**, 2659.
 BENNISON, S. J., RÖDEL, J., LATHABAI, S., CHANTIKUL, P., and LAWN, B. R., 1991, *Toughening Mechanisms in Quasi-Brittle Materials*, edited by S. P. Shah (Dordrecht: Kluwer), p. 209.
 BRAUN, L. M., BENNISON, S. J., and LAWN, B. R., 1992a, *J. Am. Ceram. Soc.*, **75**, 3049; 1992b, *Ceramic Engineering and Science Proceedings*, Vol. 13 (Westerville, Ohio: The American Ceramic Society), p. 156.
 CANNON, R. M., 1984, *Advances in Ceramics Structure and Properties of MgO and Al₂O₃ Ceramics*, edited by W. D. Kingery (Columbus, Ohio: The American Ceramic Society), p. 818.
 CHAN, H. M., and LAWN, B. R., 1988, *J. Am. Ceram. Soc.*, **71**, 29.
 CHANTIKUL, P., BENNISON, S. J., and LAWN, B. R., 1990, *J. Am. Ceram. Soc.*, **72**, 2419.
 CHO, S.-J., HOCKEY, B. J., LAWN, B. R., and BENNISON, S. J., 1989, *J. Am. Ceram. Soc.*, **72**, 1249.
 CHO, S.-J., MOON, H., HOCKEY, B. J., and HSU, S. M., 1992, *Acta metall.*, **40**, 185.
 FRANK, F. C., and LAWN, B. R., 1967, *Proc. R. Soc. Lond. A*, **299**, 291.
 HERTZ, H. H., 1896, *Hertz's Miscellaneous Papers* (London: Macmillan), chaps. 5, 6.
 HOCKEY, B. J., 1971, *J. Am. Ceram. Soc.*, **54**, 223.
 HOWES, V. R., 1990, *J. hard Mater.*, **1**, 95.
 JOHNSON, K. L., 1985, *Contact Mechanics* (Cambridge University Press).
 KNEHANS, R., and STEINBRECH, R. W., 1983, *Science of Ceramics*, Vol. 12, edited by P. Vincenzini (Imola, Italy: Ceramurgica), p. 613.

- LANGITAN, F. B., and LAWN, B. R., 1969, *J. appl. Phys.*, **40**, 4009.
- LATHABAI, S., MAI, Y. W., and LAWN, B. R., 1989, *J. Am. Ceram. Soc.*, **72**, 1760.
- LATHABAI, S., RÖDEL, J., and LAWN, B. R., 1991, *J. Am. Ceram. Soc.*, **74**, 1340.
- LAWN, B. R., 1968, *J. appl. Phys.*, **39**, 4828; 1993, *Fracture of Brittle Solids* (Cambridge: Cambridge University Press).
- LAWN, B. R., and MARSHALL, D. B., 1978, *Fracture Mechanics of Ceramics*, Vol. 3, edited by R. C. Bradt, D. P. H. Hasselman and F. F. Lange (New York: Plenum), p. 205.
- LAWN, B. R., PADTURE, N. P., BRAUN, L. M., and BENNISON, S. J., 1993, *J. Am. Ceram. Soc.*, in press.
- LAWN, B. R., and SWAIN, M. V., 1975, *J. Mater. Sci.*, **10**, 113.
- LAWN, B. R., WIEDERHORN, S. M., and ROBERTS, D. E., 1984, *J. mater. Sci.*, **19**, 2561.
- LAWN, B. R., and WILSHAW, T. R., 1975, *J. mater. Sci.*, **10**, 1049.
- LAWN, B. R., WILSHAW, T. R., and HARTLEY, N. E. W., 1974, *Int. J. Fract.*, **10**, 1.
- MAKINO, H., KAMIYA, N., and WADA, S., 1988, *J. mater. Sci. Lett.*, **7**, 475; 1991, *Proceedings of the First International Symposium on the Science of Engineering Ceramics*, edited by S. Kimura and K. Niihara (Koda, Japan: Aichi-Prefecture), p. 229.
- PADTURE, N. P., BENNISON, S. J., RUNYAN, J. L., RÖDEL, J., CHAN, H. M., and LAWN, B. R., 1991, *Ceramic Transactions*, Vol. 19, edited by M. D. Sacks (Westerville, Ohio: The American Ceramic Society), p. 715.
- PADTURE, N. P., RUNYAN, J. L., BENNISON, S. J., BRAUN, L. M., and LAWN, B. R., 1993, *J. Am. Ceram. Soc.* in press.
- PUTTICK, K. E., 1979, *J. Phys. D*, **12**, L19.
- REECE, M., and GUIU, F., 1991, *J. Am. Ceram. Soc.*, **74**, 148.
- RITCHIE, R. O., 1988, *Mater. Sci. Engng, A*, **103**, 15.
- SPERISEN, T., CARRY, C., and MOCELLIN, A., 1986, *Fracture Mechanics of Ceramics*, Vol. 8, edited by R. C. Bradt, A. G. Evans, D. P. H. Hasselman and F. F. Lange (New York: Plenum), p. 69.
- SURESH, S., 1991, *Fatigue of Materials* (Cambridge: Cambridge University Press).
- SWAIN, M. V., and HAGAN, J. T., 1976, *J. Phys. D*, **9**, 2201.
- SWAIN, M. V., and LAWN, B. R., 1969, *Phys. Stat. sol.*, **35**, 909.
- SWANSON, P. L., FAIRBANKS, C. J., LAWN, B. R., MAI, Y.-W., and HOCKEY, B. J., 1987, *J. Am. Ceram. Soc.*, **70**, 279.
- TABOR, D., 1951, *Hardness of Metals* (Oxford: Clarendon).